Inorganica Chimica Acta 471 (2018) 530–536

Contents lists available at ScienceDirect

Inorganica Chimica Acta

journal homepage: www.elsevier.com/locate/ica

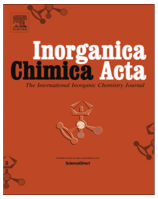

Research paper

Manganese trinuclear clusters based on schiff base: Synthesis, characterization, magnetic and electrochemiluminescence properties

Shaonan Zhang [a], Yao Hua [a,b], Zhonghang Chen [a], Shuhua Zhang [a,*], Hong Hai [a,*]

[a] College of Chemistry and Bioengineering (Collaborative Innovation Center for Exploration of Hidden Nonferrous Metal Deposits and Development of New Materials in Guangxi, Guangxi Key Laboratory of Electrochemical and Magnetochemical Functional Materials), Guilin University of Technology, Guilin 541004, PR China
[b] Qinshan Nuclear Power Plant, Jiaxin 314300, PR China

ARTICLE INFO

Article history:
Received 18 September 2017
Received in revised form 2 November 2017
Accepted 22 November 2017
Available online 23 November 2017

Keywords:
Trinuclear manganese cluster
Magnetic property
Hirshfeld surface analysis
Electrochemicaluminescence (ECL)

ABSTRACT

Four novel linear trinuclear manganese clusters $[Mn_3(L^n)_2(CH_3COO)_4]$ (**1**, n = 1; **2**, n = 2; **3**, n = 3; **4**, n = 4. where HL^1 is 4-chloro-2-((2-(6-chloropyridin-2-yl)hydrazono)methyl)phenol, HL^2 is 4-bromo-2-((2-(6-chloropyridin-2-yl)hydrazono)methyl)phenol, HL^3 is 4-chloro-2-((2-(6-bromopyridin-2-yl)hydrazono)methyl)phenol, HL^4 is 4-bromo-2-((2-(6-bromopyridin-2-yl) hydrazono)methyl)phenol) were synthesized through solvothermal method. Complexes **1**–**4** were characterized by IR, and X-ray single-crystal diffraction. Complexes **1**–**4** are isomorphous compounds which are trinuclear linear manganese clusters. A detailed analysis of Hirshfeld surface and 2D fingerprint plots revealed that **1**–**4** were supported mainly by H···H, H···X (X = Cl, Br) and O···H intermolecular interactions. Magnetic properties of **1**–**4** have been studied. In additional, complex **3** showed highly intense electrochemicaluminescence (ECL) in DMF solution.

1. Introduction

In the past decades, considerable attentions have been paid to the polynuclear complexes due to their fascinating structures and functional applications in the field of sciences and technology from fluorescent [1], optical [2], electronic [3], catalytic [4] to magnetic materials [5], as well as in the treatment and diagnosis of variety of diseases [6] and the kinds of sensors [7]. Particularly, among diverse transition polynuclear complexes, manganese complexes show fascinating properties and variable structures [8]. In fact, manganese salt is the most extensively used transition metal salt because manganese possesses variable valence state, larger spin ground states and flexible coordination modes and various coordination numbers [9]. In additional, many syntheses parameters can affect the structure and nuclear numbers of the clusters, such as metal ions, ligands, concentrations, counterions, templates, solvents, temperatures, and pH values [10].

In recent years, supramolecular chemistry is developed rapidly through using Hirshfeld surface analysis software which can analysized intermolecular interactions [11]. As a powerful tool for describing intermolecular interactions of crystal structures, Hirshfeld surface analysis can describe the surface characteristics of the molecules [12]. Hirshfeld surface analysis is the main approach to identifying the common features of crystals. Herein, we designed and synthesized four similiar schiff base ligands which constructed four similiar structure linear trinuclear manganese clusters $[Mn_3(L^n)_2(CH_3COO)_4]$ (**1**, n = 1; **2**, n = 2; **3**, n = 3; **4**, n = 4). At the same time, we study the difference of the intermolecular interactions when the substituents of the ligands are different.

2. Experimental section

2.1. Materials and instrumentation

All chemicals and solvents used for synthesis were commercially available without further purification. FT-IR spectra were recorded from KBr pellets in the range of 4000–400 cm^{-1} on a Bio-Rad FTS-7 spectrometer. Elemental analyses (CHN) were performed using a Perkin-Elmer 240 elemental analyzer. The X-ray crystal structures were determined by Agilent G8910A CCD diffractometer using the SHELXL crystallographic software for molecular structures. The ^1H NMR spectra were recorded on a Bruker AV500 spectrometer, using tetramethylsilane (TMS) as internal standard and $CDCl_3$ as solvent. Magnetic measurements were carried out with a Quantum Design PPMS model 600 magnetometer to 5 T for **1**–**4**.

---

* Corresponding authors.
E-mail addresses: zsh720108@163.com (S. Zhang), 583776610@qq.com (H. Hai).

https://doi.org/10.1016/j.ica.2017.11.045
0020-1693/

2.2. Synthesis section

Synthesis of HL^1. A mixture of 5-chloro-2-hydroxybenzaldehyde (Hchbd, 10 mmol, 1.565 g), 2-chloro-6-hydrazinylpyridine (10 mmol, 1.436 g) and ethanol (30 ml) in a 100 mL flask-3-neck refluxed at 80 °C for 3 h. The colour of the solution was changed to yellow, and was enrichment at 80 °C for 2 h. Yellow powder had been obtained by filtration, washed with ethanol (5 mL × 3) and dried in air (yield: 2.690 g, ca. 95%, based on Hchbd). Anal. calc. for HL^1 (%): $C_{12}H_9Cl_2N_3O$ (*Mr* = 283.13), *calc.*: C, 51.09; H, 3.22; N, 14.89; Found: C, 50.94; H, 3.29; N, 14.93. IR data for HL^1 (KBr, cm^{-1}, Fig. S1): 3453, 3292, 1586, 1529, 1482, 1430, 1380, 1316, 1259, 1189, 1122, 979, 930, 888, 835, 777, 703, 647, 517. ^1H NMR ($CDCl_3$, Fig. S2): δ 11.30 (s, 1H), 10.45 (s, 1H), 8.26 (s, 1H), 7.70 (d, *J* = 2.6 Hz, 1H), 7.66 (t, *J* = 7.9 Hz, 1H), 7.20 (dd, *J* = 8.7, 2.7 Hz, 1H), 7.12 (d, *J* = 8.2 Hz, 1H), 6.91 (d, *J* = 8.7 Hz, 1H), 6.81 (d, *J* = 7.5 Hz, 1H).

Synthesis of HL^2. HL^2 was synthesized by a similar way to HL^1 (Scheme 1), except that 5-chloro-2-hydroxybenzaldehyde was replaced by 5-bromo-2-hydroxybenzaldehyde (Hbhbd). Yellow powder had been obtained by filtration, washed with ethanol (5 mL × 3) and dried in air (yield: 3.168 g, ca. 97%, based on Hbhbd). *Anal. calc.* for HL^2 (%): $C_{12}H_9BrClN_3O$ (*Mr* = 326.58), *calc.*: C, 44.13; H, 2.78; N, 12.87; Found: C, 44.02; H, 2.86; N, 12.93. IR data for HL^2 (KBr, cm^{-1}, Fig. S3): 3451, 3291, 1585, 1529, 1482, 1430, 1380, 1315, 1259, 1191, 1123, 979, 931, 887, 835, 777, 702, 517. ^1H NMR ($CDCl_3$, Fig. S4): δ 11.36 (s, 1H), 10.44 (s, 1H), 8.25 (s, 1H), 7.70 (d, *J* = 2.6 Hz, 1H), 7.56 (t, *J* = 7.9 Hz, 1H), 7.21 (dd, *J* = 8.7, 2.7 Hz, 1H), 7.16 (d, *J* = 8.2 Hz, 1H), 6.95 (d, *J* = 7.5 Hz, 1H), 6.91 (d, *J* = 8.7 Hz, 1H).

Synthesis of HL^3. HL^3 was synthesized by a similar way to HL^1 (Scheme 1), except that 2-chloro-6-hydrazinylpyridine was replaced by 2-bromo-6-hydrazinylpyridine. Yellow powder had been obtained by filtration, washed with ethanol (5 mL × 3) and dried in air (yield: 3.076 g, ca. 94.2%, based on Hchbd). *Anal. calc.* for HL^3 (%): $C_{12}H_9BrClN_3O$ (*Mr* = 326.58), *calc.*: C, 44.13; H, 2.78; N, 12.87; Found: C, 44.04; H, 2.84; N, 12.95. IR data for HL^3 (KBr, cm^{-1}, Fig. S5): 3444, 3288, 3052, 1578, 1527, 1482, 1423, 1314, 1257, 1183, 1147, 1104, 974, 931, 875, 827, 776, 646, 521. ^1H NMR ($CDCl_3$, Fig. S6): δ 11.36 (s, 1H), 10.44 (s, 1H), 8.25 (s, 1H), 7.70 (d, *J* = 2.6 Hz, 1H), 7.56 (t, *J* = 7.9 Hz, 1H), 7.21 (dd, *J* = 8.7, 2.7 Hz, 1H), 7.16 (d, *J* = 8.2 Hz, 1H), 6.95 (d, *J* = 7.5 Hz, 1H), 6.91 (d, *J* = 8.7 Hz, 1H).

Synthesis of HL^4. HL^4 was synthesized by a similar way to HL^3 (Scheme 1), except that 5-chloro-2-hydroxybenzaldehyde was replaced by 5-bromo-2-hydroxybenzaldehyde. Yellow powder had been obtained by filtration, washed with ethanol (5 mL × 3) and dried in air (yield: 3.076 g, ca. 94.2%, based on Hbhbd). *Anal. calc.* for HL^4 (%): $C_{12}H_9Br_2N_3O$ (*Mr* = 371.03), *calc.*: C, 38.85; H, 2.44; N, 11.33; Found: C, 38.77; H, 2.51; N, 11.42. IR data for HL^4 (KBr, cm^{-1}, Fig. S7): 3447, 3288, 3052, 1583, 1526, 1479, 1425, 1373, 1318, 1258, 1209, 1182, 1106, 976, 925, 871, 825, 776, 691, 640, 520. ^1H NMR ($CDCl_3$, Fig. S8): δ 11.35 (s, 1H), 10.46 (s, 1H), 8.24 (s, 1H), 7.82 (d, *J* = 2.5 Hz, 1H), 7.56 (t, *J* = 7.9 Hz, 1H), 7.32 (dd, *J* = 8.7, 2.5 Hz, 1H), 7.15 (d, *J* = 8.2 Hz, 1H), 6.95 (d, *J* = 7.5 Hz, 1H), 6.86 (d, *J* = 8.7 Hz, 1H).

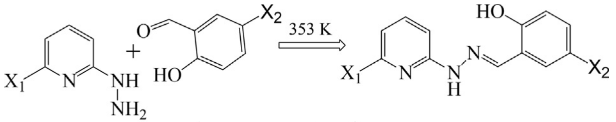

HL^1, $X_1 = X_2 = Cl$; HL^2, $X_1 = Cl$, $X_2 = Br$;
HL^4, $X_1 = X_2 = Br$; HL^3, $X_1 = Br$, $X_2 = Cl$;

Scheme 1. Structures of HL^1-HL^4.

Synthesis of $[Mn_3(L^1)_2(CH_3COO)_4]$ (1). A mixture of HL^1 (0.5 mmol, 0.141 g), $Mn(CH_3COO)_2\cdot4H_2O$ (0.5 mmol, 0.123 g), ethanol (5 mL) and DMF (5 mL) with a pH adjusted to 7 by addition of triethylamine was stirred for 20 min. The mixture was poured into a Teflon-lined autoclave (15 mL) and then heated at 80 °C for 3 days and cooled to room temperature slowly. Yellow crystals of **1** were obtained (Yield: 0.105 g, *ca.* 65.4% based on Mn). *Anal. Calc.* for **1**: $C_{32}H_{28}Cl_4Mn_3N_6O_{10}$ (*Mr* = 963.22), *calc*: C, 39.90; H, 2.97; N, 8.72%; Found: C, 39.84; H, 3.06; N, 8.80%. IR data for **1** (KBr, cm^{-1}, Fig. S1): 3449, 1621, 1532, 1463, 1391, 1298, 1251, 1171, 1117, 998, 811, 776, 728, 648.

Synthesis of $[Mn_3(L^2)_2(CH_3COO)_4]$ (2). Complex **2** was synthesized by a similar way to **1**, except that HL^1 was replaced by HL^2. Yellow crystals of **2** were obtained (Yield: 0.116 g, ca. 66.15% based on Mn). *Anal. Calc.* for **2**: $C_{32}H_{28}Br_2Cl_2Mn_3N_6O_{10}$ (Mr = 1052.14), *calc*: C, 36.53; H, 2.68; N, 7.98%; Found: C, 36.38; H, 2.79; N, 8.05%. IR data for **2** (KBr, cm^{-1}, Fig. S3): 3441, 1614, 1531, 1461, 1418, 1298, 1215, 1171, 1117, 998, 860, 778, 724, 661.

Synthesis of $[Mn_3(L^3)_2(CH_3COO)_4]$ (3). Complex **3** was synthesized by a similar way to **1**, except that HL^1 was replaced by HL^3. Yellow crystals of **3** were obtained (Yield: 0.123 g, ca. 70.14% based on Mn). *Anal. Calc.* for **3**:$C_{32}H_{28}Br_2Cl_2Mn_3N_6O_{10}$ (Mr = 1052.14), calc: C, 36.53; H, 2.68; N, 7.98%; Found: C, 36.46; H, 2.75; N, 8.03%. IR data for **3** (KBr, cm^{-1}, Fig. S5): 3424, 3218, 1616, 1567, 1462, 1344, 1296, 1253, 1170, 1114, 993, 821, 804, 775, 726, 661.

Synthesis of $[Mn_3(L^4)_2(CH_3COO)_4]$ (4). Complex **4** was synthesized by a similar way to **1**, except that HL^1 was replaced by HL^4. Yellow crystals of **4** were obtained (Yield: 0.131 g, *ca.* 68.88% based on Mn). *Anal. Calc.* For 4:$C_{32}H_{28}Br_4Mn_3N_6O_{10}$ (Mr = 1141.06), calc: C, 33.65; H, 2.45; N, 7.36%; Found: C, 33.57; H, 2.59; N, 7.39%. IR data for **4** (KBr, cm^{-1}, Fig. S7): 3426, 3221, 1616, 1537, 1462, 1343, 1295, 1254, 1171, 1113, 1047, 1019, 993, 957, 822, 802, 776, 710, 662.

2.3. Crystal structure determination

The diffraction data were collected on an Agilent G8910A CCD diffractometer with graphite monochromatic *Mo-Kα* radiation (λ = 0.71073 Å), using the ω-θ scan mode in the ranges $3.65° \le \theta \le 25.10°$ (**1**), $3.59° \le \theta \le 25.01°$ (**2**), $3.64° \le \theta \le 25.10°$ (**3**), and $358° \le \theta \le 25.10°$ (**4**). Raw frame data were integrated with the SAINT program [13]. The structures were solved by direct methods using SHELXS-97 and refined by full matrix least-squares on F2 using SHELXS-97 [13]. An empirical absorption corrections were applied with the program SADABS [13]. All non-hydrogen atoms were refined anisotropically. All hydrogen atoms were positioned geometrically and refined as riding. Calculations and graphics were performed with SHELXTL [13]. The highest peak with 1.180 $eÅ^{-3}$ and deepest hole with −1.283 $eÅ^{-3}$ of **2** in the residual electron density are located 1.08 Å from atom Br1 and 0.96 Å from atom Br1, respectively. Selected bond lengths and angles for **1**–**4** are listed in Table S1. The crystallographic details of **1**–**4** are provided in Table S2.

2.4. Hirshfeld surface calculations of 1–4

Molecular Hirshfeld surface calculations were performed by using the CrystalExplorer program [14]. When the CIF file of **1**–**4** are read into the CrystalExplorer program, all bond lengths to hydrogen were automatically modified to typical standard neutron values (C—H = 1.083 Å, N—H = 1.009 Å and O—H = 0.983 Å) [15]. In this study, all the Hirshfeld surfaces were generated using a high (standard) surface resolution. The 3D *d*norm surfaces were mapped by using a fixed colour scale of 0.76 (red) to 2.4 (blue). The 2D fingerprint plots were displayed by using the standard 0.4–2.6 Å view with the *de* and *di* distance scales displayed on the graph axes.